The Journal of Clinical Endocrinology & Metabolism, 2022, **XX**, 1–13
https://doi.org/10.1210/clinem/dgac148
Advance access publication 17 March 2022
Clinical Research Article

Associations of Abdominal and Cardiovascular Adipose Tissue Depots With HDL Metrics in Midlife Women: the SWAN Study

Alexis Nasr,[1] Karen Matthews,[1,2] Imke Janssen,[3] Maria M. Brooks,[1] Emma Barinas-Mitchell,[1] Trevor J. Orchard,[1] Jeffrey Billheimer,[4] Norman C. Wang,[5] Dan McConnell,[6] Daniel J. Rader, and[4] Samar R. El Khoudary[1]

[1]Department of Epidemiology, University of Pittsburgh, School of Public Health, Pittsburgh, Pennsylvania 15260, USA
[2]Department of Psychiatry, University of Pittsburgh School of Medicine, Pittsburgh, Pennsylvania 15213, USA
[3]Department of Preventive Medicine, Rush University Medical Center, Chicago, Illinois 60612, USA
[4]Departments of Medicine and Genetics, University of Pennsylvania Perelman School of Medicine, Philadelphia, Pennsylvania 19104, USA
[5]Division of Cardiology, Department of Medicine, University of Pittsburgh School of Medicine, Pittsburgh, Pennsylvania 15213, USA
[6]Department of Epidemiology, University of Michigan, Ann Arbor, Michigan 48109, USA

Correspondence: Samar R. El Khoudary, PhD, MPH, Department of Epidemiology, Clinical and Translational Science Institute, Epidemiology Data Center, 4420 Bayard St, Ste 600, Pittsburgh, PA 15260, USA. Email: elkhoudarys@edc.pitt.edu.

Abstract

Context: The menopause transition is accompanied by declines in the atheroprotective features of high-density lipoprotein (HDL), which are linked to deleterious cardiovascular (CV) outcomes.

Objective: This work aimed to assess the relationship between abdominal and CV visceral adipose tissues (VAT) with future HDL metrics in midlife women, and the role of insulin resistance (IR) on these associations.

Methods: Temporal associations compared abdominal and CV fat with later measures of HDL metrics. This community-based cohort comprised 299 women, baseline mean age 51.1 years (SD: 2.8 years), 67% White, 33% Black, from the Study of Women's Health Across the Nation (SWAN) HDL ancillary study. Exposures included volumes of abdominal VAT, epicardial AT (EAT), paracardial AT (PAT), or perivascular AT (PVAT). Main outcomes included HDL cholesterol efflux capacity (HDL-CEC); HDL phospholipids (HDL-PL), triglycerides (HDL-Tgs), and cholesterol (HDL-C); apolipoprotein A-I (ApoA-I), and HDL particles (HDL-P) and size.

Results: In multivariable models, higher abdominal VAT was associated with lower HDL-CEC, HDL-PL, HDL-C, and large HDL-P and smaller HDL size. Higher PAT was associated with lower HDL-PL, HDL-C, and large HDL-P and smaller HDL size. Higher EAT was associated with higher small HDL-P. Higher PVAT volume was associated with lower HDL-CEC. The Homeostatic Model Assessment of Insulin Resistance partially mediated the associations between abdominal AT depots with HDL-CEC, HDL-C, large HDL-P, and HDL size; between PVAT with HDL-CEC; and PAT with HDL-C, large HDL-P, and HDL size.

Conclusion: In midlife women, higher VAT volumes predict HDL metrics 2 years later in life, possibly linking them to future CV disease. Managing IR may preclude the unfavorable effect of visceral fat on HDL metrics.

Key Words: abdominal visceral fat, cardiovascular fat, high-density lipoproteins, midlife women

Abbreviations: ApoA-I, apolipoprotein A-I; ApoB, apolipoprotein B; AT, adipose tissue; BMI, body mass index; CETP, cholesterol ester transfer protein; CVD, cardiovascular disease; EAT, epicardial adipose tissue; EBCT, electron beam computed tomography; HDL-C, high-density lipoprotein cholesterol; HDL-CEC, high-density lipoprotein cholesterol efflux capacity; HDL-P, high-density lipoprotein cholesterol particles; HDL-PL, high-density lipoprotein cholesterol phospholipids; HDL-Tgs, high-density lipoprotein cholesterol triglycerides; HL, hepatic lipase; HOMA-IR, Homeostatic Model Assessment of Insulin Resistance; IR, insulin resistance; LCAT, lecithin-cholesterol acyltransferase; LDL-C, low-density lipoprotein cholesterol; MRL, medical research laboratory; MT, menopause transition; NMR, nuclear magnetic resonance; PAT, paracardial adipose tissue; PVAT, perivascular aortic adipose tissue; SWAN, Study of Women's Health Across the Nation; Tgs, triglycerides; VAT, visceral adipose tissue.

The 2020 American Heart Association Scientific Statement on "Menopause transition and cardiovascular disease risk: implications for timing of early prevention" highlighted the detrimental role of the menopause transition (MT) on cardiovascular disease (CVD) risk in women (1). This statement emphasized the importance of understanding the deleterious changes in CVD risk factors that accompany this vulnerable period in women's lives (1).

The MT has been linked to unfavorable changes in cardiometabolic risk factors related to lipids, metabolic syndrome, vascular health, and adipose tissue (AT) distribution (1). Alterations in the lipoprotein profile, as evidenced by increases in total cholesterol and low-density lipoprotein cholesterol (LDL-C), occur as women progress through menopause (2). However, the effect of the MT on high-density

Received: 29 November 2021. **Editorial Decision:** 6 March 2022. **Corrected and Typeset:** 6 April 2022

lipoproteins (HDLs) is more complex and the findings from earlier studies are conflicting (3).

The major antiatherogenic function of HDL is mediated by the efflux of cholesterol from macrophages through a process called reverse cholesterol transport (4, 5). The well-known atheroprotective abilities of HDL may be compromised during the MT, and levels of HDL-cholesterol (HDL-C) during and after the MT may not fully reflect those changes (6). Recent studies suggest that more novel metrics, which evaluate the function, lipid contents, and subclasses of HDL, may provide a better understanding of the alterations in the cardioprotective functions of the HDL that occur as women progress through menopause. Findings from the Study of Women's Health Across the Nation (SWAN) HDL ancillary study and Multi-Ethnic Study of Atherosclerosis (MESA) suggest that despite increases in HDL-C over the MT, adverse changes in HDL function, composition, and subclass distribution may occur, indicating a potential dysfunctionality in HDL during midlife (6, 7). For instance, the SWAN HDL ancillary study reported that the triglyceride (Tg) content of HDL increases over the MT as HDL function declines per particle (P), and that the subclass distribution shifts toward smaller Ps (6). These features have been linked to higher CVD risk profile in multiple (8-11), yet not all (12, 13), studies.

The MT is also accompanied by redistribution of AT depots (14), as characterized by increased accumulation of visceral AT, independent of weight gain. The accumulation of abdominal visceral AT (VAT) in women peaks during the perimenopausal stage (15); this has been linked to elevated future risk of subclinical atherosclerosis (15). Beyond the abdomen, VAT accumulation extends to ectopic locations in the body such as the heart. Similar to abdominal VAT, postmenopausal women have higher volumes of cardiovascular AT, particularly paracardial fat (PAT) (16), and this is associated with higher risk of coronary artery calcification in postmenopausal women (17).

VAT plays a role in the regulation of lipid metabolism including that of the HDL. In midlife and older women, higher abdominal VAT is linked to lower levels of HDL-C (18). However, no studies have assessed how VAT is associated with the function, composition, and size of HDL in women during midlife. Understanding the link between VAT and HDL metrics could help delineate the metabolic consequences of VAT accumulation and understand how VAT could affect future CVD risk in women, specifically during the vulnerable midlife period. Since VAT accumulation is often accompanied by a state of insulin resistance (IR) that can, in turn, contribute to HDL metabolism through several lipoprotein-related enzymes (19, 20), it is important to understand the role of IR on the associations between VAT depots and HDL metrics.

The SWAN Heart, Cardiovascular Fat, and HDL ancillary studies provide a unique opportunity to assess the temporal associations between different AT depots and a future comprehensive HDL metric profile in midlife women. In this study, we evaluate the relationship between VAT depots and HDL metrics measured 2 years later on average in White and Black midlife women, and investigate the mediation effect of IR on those associations. We hypothesize that higher volumes of abdominal and CV AT will be associated with a worse HDL metric profile (lower HDL function, higher Tg and lower PL contents, and with smaller HDL subclasses and overall size). IR will mediate these associations in such a way that higher VAT will be associated with more IR and, thus, a worse HDL profile.

Materials and Methods

SWAN is an ongoing, multisite, multiethnic, community-based, longitudinal study that aims to characterize the physiological and psychological changes in women as they traverse menopause. The design of the SWAN study has been previously described (21). Briefly, 3302 women aged 42 to 52 years were recruited between 1996 and 1997 at seven different sites across the United States (Pittsburgh, Pennsylvania; Chicago, Illinois; Boston, Massachusetts; Newark, New Jersey; Detroit, Michigan; Los Angeles, California; and Oakland, California). Eligibility criteria for recruitment into SWAN were (i) having an intact uterus and at least one ovary, (ii) not being pregnant or lactating at recruitment time, (iii) having had at least one menstrual period within the last 3 months before recruitment, (iv) not using hormone therapy, and (v) identifying as White, Black, Hispanic, Chinese, or Japanese.

The SWAN HDL study is an ancillary study to SWAN. This study aims to characterize the biological changes in HDL composition and function that accompany ovarian aging, and to identify how these changes influence the atheroprotective capacities of HDL in women. For the SWAN HDL study, frozen serum samples from 558 SWAN women at different SWAN visits (1461 samples) were used to quantify HDL function, lipid content, and subclasses. Women were selected into SWAN HDL if they had participated in at least 1 visit before and at least 2 visits after the final menstrual period, with available blood samples at the selected visits (6). The SWAN Heart ancillary study aimed to evaluate subclinical atherosclerosis in SWAN participants at the Chicago and Pittsburgh sites; the SWAN Cardiovascular Fat ancillary study measured CV fat in SWAN Heart study participants who had electron beam computed tomography (EBCT) scans available at the SWAN Heart baseline visit (16).

For this study, we performed a prospective analysis in which each of the exposures (VAT depots) was measured at 1 visit (coinciding with SWAN follow-up visits 4-7) and each outcome (HDL metrics) was measured at a later visit (coinciding with SWAN follow-up visits 5-7, 9, or 12) (Fig. 1A). Women who had missing data on all AT measures (abdominal VAT, epicardial AT [EAT], PAT, and perivascular aortic AT [PVAT]) were excluded. We included 299 women who had any AT measure (abdominal VAT, EAT, PAT, or PVAT) followed by a later HDL metrics measure (HDL cholesterol efflux capacity [HDL-CEC], HDL lipid contents, HDL subclasses, HDL size, HDL-C, and apolipoprotein A-I [ApoA-I]). For each woman, one HDL metric measure was selected after the AT measure. The median duration between the assessment of AT and HDL metrics was 2.0 years (Q1: 1.8 years to Q3: 2.2 years). Compared to excluded women (n = 259), the included women had higher body mass index; BMI. Age, physical activity score, antilipid medication use, and Homeostatic Model Assessment of Insulin Resistance (HOMA-IR) were similar between groups. All participants provided written informed consent at every study SWAN visit, and study protocols were approved by the institutional review board at each study site.

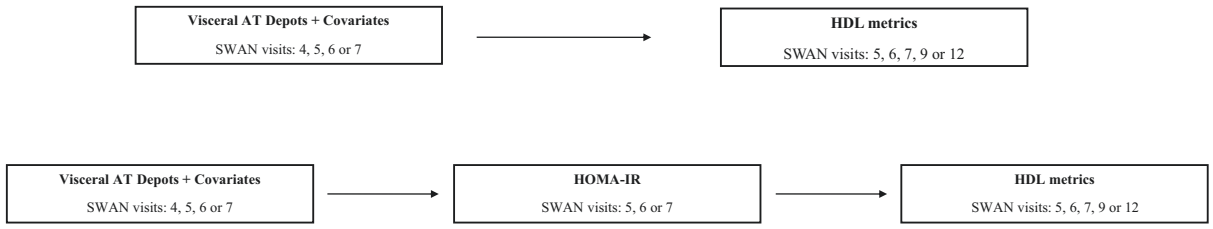

Figure 1. A, Timeline for data collection of variables for analysis of associations between visceral adipose tissue (AT) depots and high-density lipoprotein (HDL) metrics. B, Timeline for data collection of variables for analysis of mediation of the Homeostatic Model Assessment of Insulin Resistance (HOMA-IR) on associations between visceral AT depots and HDL metrics.

Measures of Visceral Adipose Tissue Depots

Abdominal visceral adipose tissue

The GE-Imatron C150 EBCT Scanner (GE Medical Systems) was used to quantify abdominal AT volume within a single 6-mm-thick cross-sectional image between the L4 and L5 vertebral space (22). Scans were read by a single reader at the University of Pittsburgh. AT was distinguished from other tissues of the abdomen by the threshold of –190 to –30 Hounsfield units (HU) by methods of image analysis software (AcuImage Software). A line was drawn along the fascial plane at the interior of the abdominal muscles, and fat within this line was considered VAT. Intraobserver reliability for abdominal VAT quantification was reported with an intraclass coefficient of 0.94 (22).

Cardiovascular adipose tissue

EAT and PAT adipose tissues were quantified on images that were previously acquired for the measurement of coronary artery calcification (16). The images were obtained by the GE-Imatron C150 EBCT Scanner (GE Medical Systems) (16). For EAT and PAT, 3-mm-thick transverse images were read at the Los Angeles Biomedical Research Institute, Harbor–UCLA Medical Center, California, USA. EAT and PAT areas were determined between 15 mm above and 30 mm below the superior extent of the left main coronary artery, which allowed for the evaluation of fat around the proximal coronary arteries. The chest wall was the landmark for the anterior border, and the aorta and bronchus were the landmarks for the posterior border. AT was distinguished from other tissues of the heart by the threshold of –190 to –30 HU by methods of volume analysis software (GE Healthcare). EAT and PAT were measured manually by tracing the border of the area of interest every 2 to 3 CT slices and using the software to automatically trace the slices in between. EAT volume was defined as the fat inside the pericardium, and PAT was defined as the fat outside of the pericardium. PAT volume was calculated by subtracting the EAT volume from the total cardiac fat volume. The between- and within-reader Spearman correlation coefficients for EAT and PAT volumes were 0.97 (16).

To quantify perivascular aortic AT (PVAT) volume, 6-mm-thick transverse images that were previously obtained for evaluation of aortic calcification were read at the University of Pittsburgh Ultrasound Research Laboratory with Slice-O-Matic version 4.3 software (Tomovision) (16). PVAT was defined as the adipose tissue surrounding the descending aorta. The pulmonary bifurcation was the landmark to determine the proximal border, the first lumbar vertebrae was the landmark for the distal border, the vertebral foramen was the landmark for the posterior border, and the line crossing through the left bronchus to the interior border of the crus of the diaphragm was the anterior border. PVAT was distinguished from other surrounding tissue by a –190 to –30 HU threshold. The borders were identified manually for every slice. Since the length of the evaluated part of the descending aorta varies across participants, the length of the descending aorta was estimated from table position number at first included CT slice and table position number at last included CT slice, and accounted for in multivariable analysis. The between- and within-reader Spearman correlation coefficients for PVAT volumes were 0.998 and 0.999, respectively (23).

All readers of the cardiovascular AT depots at the Los Angeles Biomedical Research Institute and the University of Pittsburgh Ultrasound Research Laboratory were blinded to the participants' characteristics.

Blood Data Collection

Phlebotomy was performed after a minimum of a 10-hour overnight fast. This was scheduled 2 to 5 days after a spontaneous menstrual bleed when possible. When menstrual cycles were less predictable, phlebotomy was randomly performed within 90 days of the annual SWAN visit. Stored samples that have been frozen at –80 °C and never been thawed were used for SWAN HDL assays to guarantee the validity of results.

Cholesterol efflux capacity and lipid content of high-density lipoprotein

HDL-CEC, HDL-PL, and HDL-Tgs were measured at a Centers for Disease Control and Prevention–certified lipid laboratory at the University of Pennsylvania. HDL-CEC was measured by the efflux of fluorescence-labeled cholesterol as has been described previously (9). Briefly, J774 mouse macrophage cells were plated and labeled with 2 μCi/mL of ^{3}H cholesterol overnight. The cells were then incubated in the presence of 0.3 mM 8-(4-chlorophenylthio)-cyclic adenosine 5′-monophosphate (cAMP), an upregulator of adenosine 5′-triphosphate–binding cassette transporter-1 (ABCA1), for 4 hours. Lipoproteins containing apolipoprotein B (ApoB) were removed from plasma by polyethylene glycol precipitation, resulting in ApoB-depleted serum. The cells were then incubated with the equivalent of 1% ApoB-depleted serum or plasma for 2 hours at a temperature of 37 °C. Cells incubated with media alone were used as baseline controls. Each medium was then collected and passed through a 0.22-μM filter to remove cell debris. Isopropanol extraction was then used to extract lipids from cells. ^{3}H cholesterol was quantitated in media and cells by scintillation counting. Percentage efflux capacity was calculated by the following formula: [(cpm of ^{3}H cholesterol in the media – cpm of ^{3}H cholesterol in serum free

media)/(cpm of ^{3}H cholesterol in the cells + cpm of ^{3}H cholesterol in the media)] × 100. The intra-assay and interassay coefficients of variation were 3.7% and 10.1%, respectively.

For HDL-PL and HDL-Tg quantification, HDL was isolated from serum by phosphotungstic acid precipitation (FujiFilm Wako Pure Chemical Corporation) and HDL-PL and HDL-Tg were measured by the Roche Cobas C311 clinical analyzer according to manufacturer's protocol (Wako: 433-36201 and Roche: 20767107322, respectively). The interassay coefficients of variation were 3.5% and 3.9% for HDL-PL and HDL-Tg, respectively.

High-density lipoprotein subclasses

HDL subclasses and size were measured at LabCorp by the nuclear magnetic resonance (NMR) spectroscopy LipoProfile-3 algorithm (24), by the Vantera Clinical Analyzer, which is an automated 400 MHz NMR spectroscopy platform. In brief, lipoprotein P quantification by NMR uses composite signal envelopes at 0.8 ppm, which contain the signals emitted by terminal methyl group protons of the PLs, unesterified cholesterol, cholesterol ester, and Tgs that are carried in each HDL lipoprotein P. Signal amplitudes that contribute to the composite plasma signal are produced as a result of the deconvolution of the composite signal. Each lipoprotein subclass produces unique NMR signals that are specific in frequency and shape. The amplitude of the signal is proportional to the number of Ps that are releasing the signal.

To obtain the amplitude of each subpopulation of subclasses, the line shape of the signal envelope was modeled as a sum of all lipoprotein signals. The areas of different subpopulations were multiplied by conversion factors to quantify the concentrations, which were then grouped into small (7.3-8.2 nm), medium (8.2-9.4 nm), or large (9.4-14.0 nm) HDL subclasses. The total HDL-P concentration was obtained by summing the concentrations of all subclasses. The average size of HDL Ps was calculated by adding the diameter of each subclass multiplied by its relative mass percentage from NMR signal amplitude. Owing to the magnetic property of lipoproteins that produces signals of different shapes and frequencies for different lipoproteins, NMR spectroscopy does not require the separation of lipoprotein subclasses as is required by electrophoresis or ultracentrifugation.

The intra-assay and inter-assay coefficients of variation for HDL-P concentrations and size ranged from 0.6% to 3.7% (intra-assay) and 1.5% to 4.0% (interassay).

High-density lipoprotein cholesterol and apolipoprotein A-I

Lipid fractions were determined in EDTA-treated plasma. Fasting HDL-C (25, 26) was separated with heparin-2M manganese chloride (Medical Research Laboratory, Lexington, Kentucky, for SWAN baseline visit until follow-up visit 7; University of Michigan Pathology, Ann Arbor, Michigan, at SWAN follow-up visits 9 and 12). HDL-C was calibrated by converting the results at SWAN visits 9 and 12 to equivalent medical research laboratory (MRL) values.

ApoA-I was quantified by the immunonephelometry using Behring reagents on the Behring Nephelometer II at MRL between SWAN baseline visit and follow-up visit 7, and by reagents from Beckman-Coulter at the University of Pittsburgh Heinz laboratory at SWAN visits 9 and 12. ApoA-I results from the University of Pittsburgh were calibrated by converting to equivalent MRL values.

Study Covariates

Race and economic hardship were self-reported at the SWAN baseline visit. Economic hardship was defined as difficulty paying for basics (not hard or somewhat/very hard). Other study covariates were measured at the time of AT depot assessment. Age was calculated as the difference between the visit date at which AT was assessed and the date of birth. BMI was calculated as measured weight in kilograms divided by the square of height in meters. Physical activity score was measured by the Modified Kaiser Permanente Health Plan Activity Survey (27). Menopause status was self-reported at every SWAN visit and categorized based on bleeding patterns over the past 12 months. Menopause status was classified as either premenopausal/early-perimenopausal (no changes in menstrual bleeding patterns over the past 12 months, or at least 1 bleed within the last 3 months with some perceived changes in menstrual cycle intervals), late perimenopausal/postmenopausal (no bleed within the past 3 months but at least 1 cycle within the last 12 months, or lack of menstrual bleeding for 12 or more consecutive months, either naturally or surgically due to bilateral salpingo-oophorectomy), or unknown menopause status (due to hysterectomy or hormone therapy use). Tg levels were analyzed in plasma at the MRL by an automated glycerol kinase enzymatic assay on a Hitachi 747-200 clinical analyzer. HOMA-IR was calculated as fasting glucose (mg/dL) × fasting insulin (mIU/mL)/405.

Statistical Analysis

Descriptive statistics using mean (SD), median (Q1-Q3), or frequencies (%) were used to summarize participants' characteristics at the time of AT assessments. The distribution of continuous variables was assessed, and skewed variables (abdominal VAT, PAT, EAT, PVAT, HDL-Tgs, large HDL-P, medium HDL-P, Tgs, and HOMA-IR) were log-transformed to reduce skewness. Correlations between different AT depots were tested by Spearman correlations.

Lagged analyses were used to assess the relation between different VAT volumes in relation to future HDL metrics, where one HDL metric measure was selected after each AT measure. Multivariable linear regression models were used to evaluate the associations between each VAT depot at one visit with each HDL metric at a later visit, separately. Variables that were univariately associated with both exposures and outcomes were considered as confounders, and the best parsimonious model was chosen by comparing models using the R-squares, without introducing multicollinearity. Final models were adjusted for race, time between the VAT and HDL metric assessment, economic hardship, and the following measures at time of AT assessment: age, physical activity, menopause status, and log-transformed Tgs. PVAT models were additionally adjusted for length of the descending aorta. Interaction between race and each HDL metric was tested in final models to assess whether associations differed between White and Black women. For graphical representation of the statistically significant associations between AT depots and HDL metrics, volumes of AT depots were categorized into tertiles, and means of HDL metrics within each tertile were estimated in the final models. Tertiles were used to ensure sufficient numbers of participants per group. Post hoc Bonferroni adjustment was applied to correct for multiple testing.

Whether IR mediated the associations between AT depots and HDL, causal mediation analysis was used to test the effect

of log-transformed HOMA-IR on these associations. To ensure temporality between exposure, mediator, and outcome, this was performed in a subset of women (n = 251) who had HOMA-IR evaluated at visits between the fat depot and HDL metrics measures, that is, after adipose tissue was evaluated but before HDL metrics were assessed (Fig. 1B). The women included in this subanalysis were similar to the excluded women (n = 48) on all characteristics (data not shown). All analyses were conducted using SAS v9.4 (SAS Institute).

Results

Characteristics of Women included in This Analysis

The characteristics of the women included in this analysis at the time of AT assessment are presented in Table 1. Women, on average, were aged 51.1 years (SD: 2.8 years), 67% were White, and 57% were premenopausal/early-perimenopausal. AT depots were measured 2.0 years (Q1: 1.8 years to Q3: 2.2 years) before HDL metrics measures.

Abdominal VAT was strongly correlated with EAT (*r*s: 0.67-0.74, all $P < .0001$). All CV AT volumes were also correlated: EAT was correlated with PAT and PVAT; PAT was correlated with PVAT (*r*s: 0.62-0.68; all $P < .0001$).

Univariate Correlations Between Abdominal and Cardiovascular Visceral Adipose Tissue Depots and High-density Lipoprotein Metrics

The univariate correlations between AT depots and HDL metrics are presented in Table 2. All AT depots were inversely correlated with HDL-PL and HDL-C, and all except EAT were inversely correlated with ApoA-I. Abdominal VAT and PVAT were negatively correlated with HDL-CEC. Abdominal VAT and EAT were positively correlated with HDL-Tgs. All AT depots were inversely correlated with large HDL-P and HDL size, and positively with small HDL-P. There were no correlations between the AT depots with total or medium HDL-P.

Associations Between Abdominal and Cardiovascular Visceral Adipose Tissue and High-density Lipoprotein Metrics

Figs. 2 and 3 present the statistically significant multivariable associations between AT depots tertiles and HDL metrics. The multivariable-adjusted associations between the AT depots and HDL function and content metrics are presented in Fig. 2. Higher PVAT tertiles were associated with borderline lower HDL-CEC (P trend = .06), whereas higher abdominal VAT volumes were associated with lower HDL-PL (P trend = .02), and higher abdominal VAT and PAT tertiles were associated with lower HDL-C (P trends = .008 and .04, respectively).

The multivariable-adjusted associations between the AT depots and HDL subclasses and size are presented in Fig. 3. Abdominal VAT and PAT tertiles were associated with lower levels of large HDL-P (P trends <.001 and .008, respectively) and smaller overall size (P trends = .004 and .001, respectively). Higher tertiles of EAT were associated with more levels of small HDL-P (P trend = .02). All other associations between the different AT depots and HDL metrics were attenuated after adjusting for potential confounders.

The adjusted associations between the 4 continuous AT depots and each HDL metric are presented in Supplementary Tables 1 and 2 and are largely consistent with the findings from the analysis by tertiles (28).

Table 1. Characteristics of women included in this analysis

Participant characteristics	N = 299
Characteristics at time of fat assessment	
Age, y, mean (SD)	51.1 (2.8)
Race, n (%)	
White	201 (67.2%)
Black	98 (32.8%)
Menopause status, n (%)	
Premenopause/Early-perimenopause	169 (56.5%)
Late-perimenopause/Postmenopause	106 (35.5%)
Unknown	24 (8.0%)
Difficulty paying for basics	
No	208 (69.6%)
Yes	91 (30.4%)
BMI, median (Q1-Q3)	27.6 (24.4-33.0)
Physical activity score, mean (SD)	7.97 (1.76)
HOMA-IR, median (Q1-Q3)	1.89 (1.42-3.06)
Triglycerides (mg/dL), median (Q1-Q3)	104 (77-143)
Abdominal VAT volume (cm^3), median (Q1-Q3)	66.3 (42.4-95.0)
EAT volume (cm^3), median (Q1-Q3)	37.0 (28.0-51.7)
PAT volume (cm^3), median (Q1-Q3)	8.5 (4.4-14.1)
PVAT volume (cm^3), median (Q1-Q3)	29.2 (23.7-37.7)
HDL measures at subsequent visit	
HDL-CEC (%), mean (SD)	3.84 (0.64)
HDL-Tg (mg/dL), median (Q1-Q3)	17 (15-21)
HDL-PL (mg/dL), mean (SD)	53.9 (10.0)
Total HDL-P (µmol/L), mean (SD)	35.4 (6.6)
Large HDL-P (µmol/L), median (Q1-Q3)	7.4 (4.9-9.6)
Medium HDL-P (µmol/L), median (Q1-Q3)	9.6 (5.6-14.4)
Small HDL-P (µmol/L), mean (SD)	17.2 (7.2)
HDL size (nm), mean (SD)	9.37 (0.56)
HDL-C (mg/dL), mean (SD)	57.3 (14.0)
ApoA-I (mg/dL), mean (SD)	165.9 (27.7)

HDL-C: 1 mg/dL = 0.0259 mmol/L; triglycerides: 1 mg/dL = 0.0113 mmol/L.
Abbreviations: ApoA-I, apolipoprotein A-I; BMI, body mass index; EAT, epicardial adipose tissue; HDL, high-density lipoprotein; HDL-C, high-density lipoprotein cholesterol; HDL-CEC, high-density lipoprotein cholesterol efflux capacity; HDL-P, high-density lipoprotein particles; HDL-PL, high-density lipoprotein phospholipids; HDL-Tg, high-density lipoprotein triglycerides; HOMA-IR, Homeostatic Model Assessment of Insulin Resistance; PAT, paracardial adipose tissue; PVAT, perivascular aortic adipose tissue; VAT, visceral adipose tissue.

After adjusting for multiple comparisons, interactions between HDL metrics and race in the final models showed that the associations did not differ between White and Black women (data not shown).

Mediation by the Homeostatic Model Assessment of Insulin Resistance on the Association Between Visceral Adipose Tissue and High-density Lipoprotein Metrics

Table 3 and Fig. 4 present the statistically significant results of the mediation analysis on the observed associations between AT depots and HDL metrics. For abdominal VAT, IR mediated 62.0% of the associations with HDL-CEC, 50.9% of the associations with HDL-C, 32.1% of the associations

Table 2. Spearman correlations between visceral adipose tissue depots and high-density lipoprotein metrics

	HDL function and contents									
	HDL-CEC, %		HDL-Tg		HDL-PL		HDL-C		ApoA-I	
AT depots	*r*	*P*	*r*	*P*	*r*	*P*	*r*	*P*	*r*	*P*
Abdominal VAT	–0.13	.03	0.17	.004	–0.26	<.001	–0.39	<.001	–0.23	<.001
EAT	–0.12	.06	0.16	.009	–0.14	.03	–0.22	<.001	–0.08	.21
PAT	–0.12	.06	0.10	.13	–0.20	.002	–0.30	<.001	–0.17	.009
PVAT	–0.13	.03	0.11	.08	–0.18	.002	–0.27	<.001	–0.17	.007
	HDL subclasses and size									
	Total HDL-P		Large HDL-P		Medium HDL-P		Small HDL-P		HDL size	
AT depots	*r*	*P*	*r*	*P*	*r*	*P*	*r*	*P*	*r*	*P*
Abdominal VAT	–0.06	.30	–0.42	<.001	–0.10	.10	0.20	<.001	–0.38	<.001
EAT	0.02	.80	–0.26	<.001	–0.11	.07	0.22	<.001	–0.24	<.001
PAT	–0.03	.68	–0.31	<.001	–0.03	.60	0.15	.01	–0.28	<.001
PVAT	–0.02	.69	–0.30	<.001	–0.02	.69	0.13	.03	–0.25	<.001

Abbreviations: ApoA-I, apolipoprotein A-I; EAT, epicardial adipose tissue; HDL-C, high-density lipoprotein cholesterol; HDL-CEC, high-density lipoprotein cholesterol efflux capacity; HDL-P, high-density lipoprotein particles; HDL-PL, high-density lipoprotein phospholipids; HDL-Tg, high-density lipoprotein triglycerides; PAT, paracardial adipose tissue; PVAT, perivascular aortic adipose tissue; VAT, visceral adipose tissue.

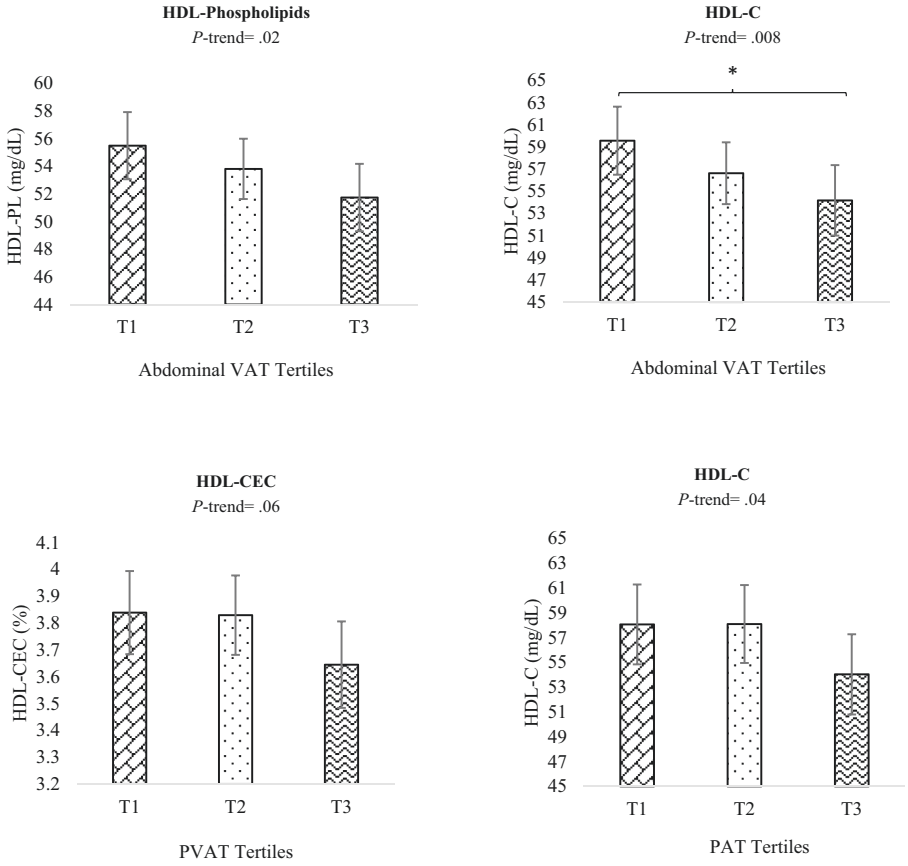

Figure 2. Associations between visceral adipose tissue (VAT) tertiles and high-density lipoprotein (HDL) function and content metrics. Models adjusted for race, time between adiposity and HDL metric assessment, economic hardship, and the following measures at time of AT assessment: age, physical activity, menopause status, and log-transformed triglycerides. Perivascular adipose tissue (PVAT) models additionally adjusted for length of the descending aorta. Bonferroni adjustments for multiple comparisons. *Groups significantly different. Abdominal VAT volume tertiles: tertile 1 (T1) ≤ 50.6 cm^3; 50.6 < tertile 2 (T2) ≤ 83.8 cm^3; tertile 3 (T3) ≥ 83.3 cm^3. PAT volume tertiles: tertile 1 (T1) ≤ 5.4 cm^3; 5.4 < tertile 2 (T2) ≤ 11.5 cm^3; tertile 3 (T3) ≥ 11.5 cm^3. PVAT volume tertiles: tertile 1 (T1) ≤ 25.5 cm^3; 25.5 < tertile 2 (T2) ≤ 34.6 cm^3; tertile 3 (T3) ≥ 34.6 cm^3.

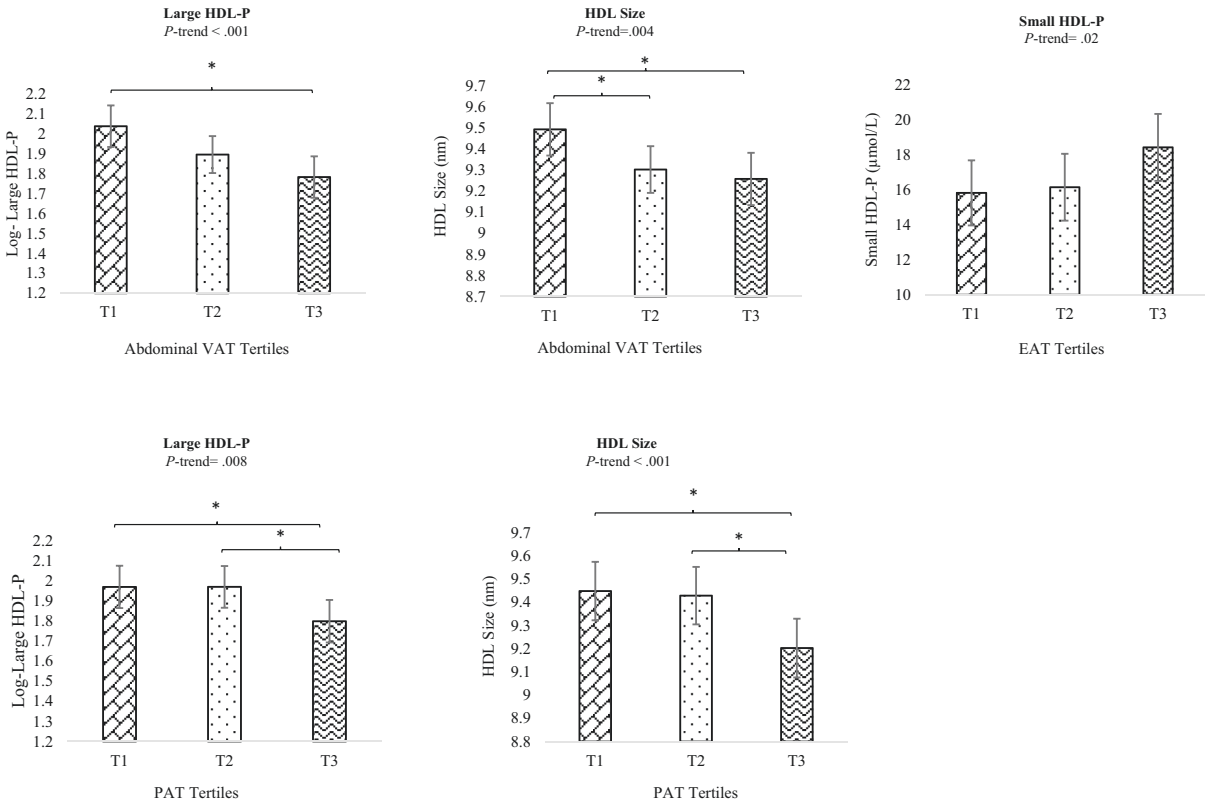

Figure 3. Associations between adipose tissue (AT) tertiles and high-density lipoprotein (HDL) subclasses and size. Models adjusted for race, time between adiposity and HDL metric assessment, economic hardship, and the following measures at time of AT assessment: age, physical activity, menopause status, and log-transformed triglycerides. Bonferroni adjustments for multiple comparisons. *Groups significantly different. Abdominal visceral adipose tissue (VAT) volume tertiles: tertile 1 (T1) ≤ 50.6 cm^3; 50.6 < Tertile 2 (T2) ≤ 83.8 cm^3; Tertile 3 (T3) ≥ 83.3 cm^3. Epicardial adipose tissue (EAT) volume tertiles: tertile 1 (T1) ≤ 31.7 cm^3; 31.7 < tertile 2 (T2) ≤ 45.1 cm^3; tertile 3 (T3) ≥ 45.1 cm^3. Paracardial adipose tissue (PAT) volume tertiles: tertile 1 (T1) ≤ 5.4 cm^3; 5.4 < tertile 2 (T2) ≤ 11.5 cm^3; tertile 3 (T3) ≥ 11.5 cm^3.

with large HDL-P, and 34.5% of associations with HDL size. For PAT, IR mediated 51.6% of the associations with HDL-C, 44.9% of associations with large HDL-P, and 37.1% of associations with HDL size. IR mediated 34.7% of the associations between PVAT and HDL-CEC. The natural indirect effect represents the effect of VAT on each HDL metric that is mediated by IR. The controlled direct effect represents how much the HDL metric would change on average if IR was fixed at a sample mean and AT depot volumes are increased by 1 unit. The controlled direct effect shows that if IR was held constant, the decrease in each of the HDL metrics (HDL-CEC, HDL-C, large HDL-P, and HDL size) with the increase in AT depots would have been less pronounced than observed in this analysis.

Discussion

In a sample of midlife women, we show that visceral fat accumulation in the abdomen and around the heart and vasculature may be linked to future dysfunction in HDL. Higher volumes of abdominal and CV AT depots were associated with lower HDL-CEC, lower HDL-PL, HDL-C, large HDL-P, and higher small HDL-P concentrations, and with smaller overall HDL size, independent of potential CV and metabolic confounders. This profile of HDL metrics has been linked to worse CV outcomes (9-11). Furthermore, IR appears to mediate and drive some of the deleterious associations between AT depots and HDL metrics, particularly the associations between AT depots with HDL-CEC, large HDL-P, and HDL size.

Only a limited number of studies had investigated the relation between abdominal VAT and novel HDL metrics. In a cross-sectional analysis of 1200 obese participants from the Dallas Heart Study, Neeland et al (29) reported that higher abdominal VAT mass was associated with smaller overall HDL size and lower HDL-C concentrations. These associations were similar for men and women. Consistent with our results, the associations did not differ by race. In another cross-sectional analysis of 382 individuals, Sam et al (30) similarly reported an inverse association between abdominal VAT and overall HDL size. In women specifically, Woudberg et al (31) followed 24 young women (mean age, 29 years [2 years]) for an average of 5.5 years and showed that an increase in abdominal VAT over time was associated with a decline in large HDL subclasses as measured by gel electrophoresis; no changes in HDL-C were observed. Nicklas et al (18) reported that perimenopausal and postmenopausal women (mean age, 59 years [SD: 6 years]) in the lowest abdominal VAT quintile had statistically significantly higher HDL-C and large HDL2-C subclasses as measured by ultracentrifugation. Results of these studies are in agreement with our findings; however, none of these studies focused on women during midlife, and none investigated whether abdominal VAT is related to composition and functional measures of HDL.

Table 3. Mediation analysis for the Homeostatic Model Assessment of Insulin Resistance on the associations between adipose tissue depots and high-density lipoprotein metrics[a]

	Natural indirect effect		Controlled direct effect		Total effects		Percentage mediated[c]
	β (SE)	*P*	β (SE)	*P*	β (SE)	*P*	
	Abdominal VAT[b]						
HDL-CEC	−0.06 (0.03)	.02	−0.04 (0.05)	.45	−0.10 (0.05)	.03	62.0%
HDL-C	−1.26 (0.55)	.02	−1.13 (1.02)	.27	−2.47 (0.89)	.006	50.9%
Large HDL-P[b]	−0.04 (0.02)	.02	−0.08 (0.03)	.03	−0.12 (0.03)	< .0001	32.1%
HDL size	−0.04 (0.02)	.03	−0.07 (0.04)	.07	−0.13 (0.03)	.0003	34.5%
	PAT[b]						
HDL-C	−0.90 (0.37)	.02	−1.05 (0.94)	.26	−1.73 (0.90)	.05	51.6%
Large HDL-P[b]	−0.03 (0.01)	.007	−0.05 (0.03)	.12	−0.08 (0.03)	.01	44.9%
HDL size	−0.04 (0.01)	.01	−0.06 (0.04)	.07	−0.09 (0.03)	.005	37.1%
	PVAT[b]						
HDL-CEC	−0.04 (0.02)	.03	−0.07 (0.05)	.12	−0.11 (0.04)	.02	34.7%

Models adjusted for race, time between adiposity and HDL metric assessment, economic hardship, and the following measures at time of adipose tissue assessment: age, physical activity, menopause status, and log-transformed triglycerides. PVAT models additionally adjusted for length of the descending aorta.
Abbreviations: HDL-C, high-density lipoprotein cholesterol; HDL-CEC, high-density lipoprotein cholesterol efflux capacity; HDL-P, high-density lipoprotein particles; PAT, paracardial adipose tissue; PVAT, perivascular aortic adipose tissue; VAT, visceral adipose tissue.
[a]We present data for significant mediation results, where the total effect is statistically significant.
[b]Log-transformed.
[c]Calculated as natural direct effect/total effects × 100%.

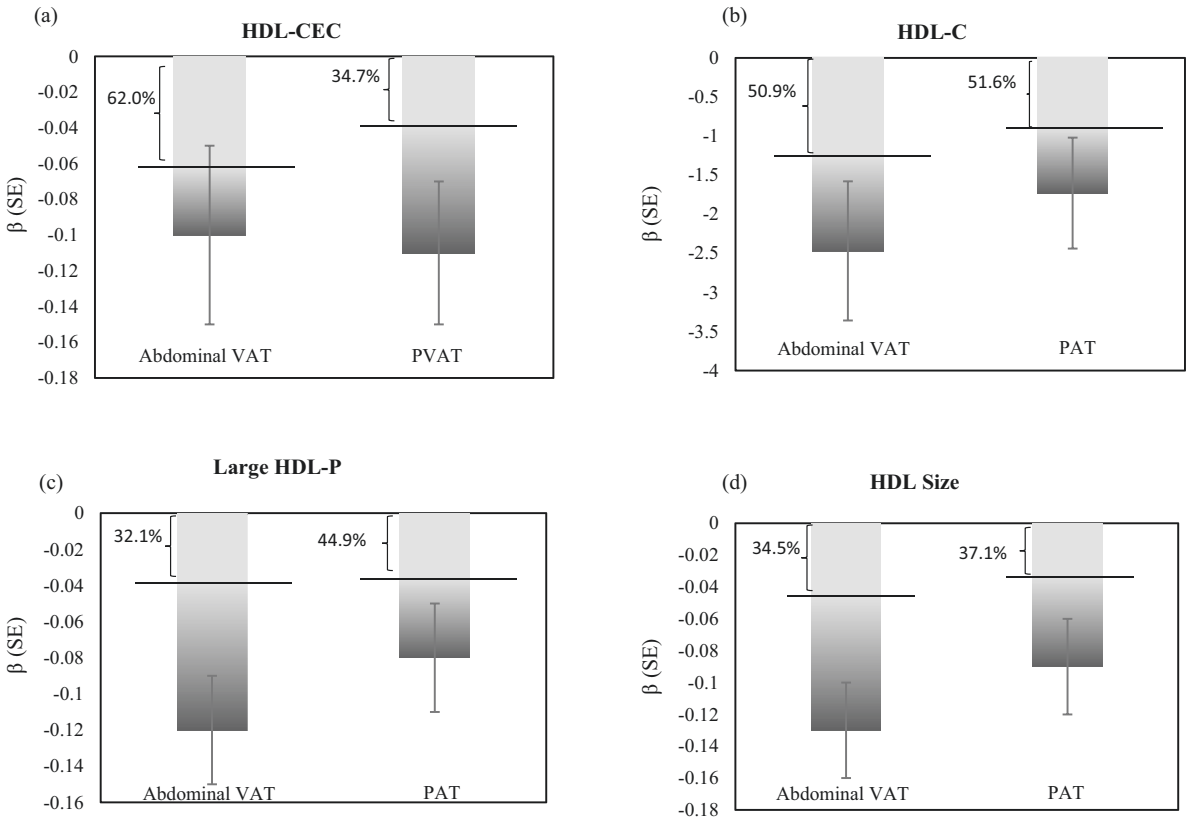

Figure 4. Mediation effect by the Homeostatic Model Assessment of Insulin Resistance (HOMA-IR) on the associations between adipose tissue (AT) depots and high-density lipoprotein (HDL) metrics. Effect of HOMA-IR as a mediator on the associations between AT depots and A, HDL-CEC; B, HDL-C; C, large HDL-P; and D, HDL size. Models adjusted for race, time between adiposity and HDL metric assessment, economic hardship, and the following measures at time of AT assessment: age, physical activity, menopause status, and log-transformed triglycerides. Perivascular adipose tissue (PVAT) models additionally adjusted for length of the descending aorta. The gray + black area represent the total effect of the association between the AT depot and the HDL metric. The gray area represents the percentage mediated by HOMA-IR (natural indirect effect/total effect × 100%).

Only a single study from the Multi-Ethnic Study of Atherosclerosis had assessed the relation between cardiovascular AT depots and HDL subclasses as measured by NMR (n = 5407, 53% women; mean age, 62.5 years) (32). Greater PAT volume, defined as the fat around the proximal coronary arteries, was associated with lower HDL-C, total, large and medium HDL-P levels, but with higher small HDL-P. Interaction by race showed that this association was statistically significant only in White participants; no interaction by sex was tested. In an analysis of 650 postmenopausal women from the KEEPS study (mean age 52.9 years [2.6 years]), Huang and colleagues (33) reported that EAT (fat inside the pericardial sac), pericardial fat (fat outside the pericardial sac), and total AT (EAT + pericardial AT) were independently and negatively associated with HDL-C.

The potential mechanism that links the different VAT depots to HDL metrics is complex. An array of enzymes that are influenced by the VAT accumulation has been proposed to be involved in the pathway linking adiposity to HDL metabolism. Hepatic lipase (HL) and cholesterol ester transfer protein (CETP) are elevated with higher VAT accumulation (34, 35). HL hydrolyzes large HDL Ps to form smaller, dense HDL (34), whereas CETP transfers Tgs from Tg-rich lipoproteins to HDL particles in exchange for cholesteryl esters (35). This leads to the formation of more Tg-rich HDL particles (36) which become favorable substrates for hepatic triglyceride lipase and eventually smaller HDL particles (37). Another enzyme that could be involved in the mechanistic link between visceral AT and HDL is the lecithin-cholesterol acyltransferase (LCAT), which esterifies free cholesterol in HDL particles and increase the size of the HDL (38). In one study that assessed the relation between obesity, as measured by BMI, with HDL metrics, it was reported that a BMI greater than 30 in young women was associated with a shift in HDL subclasses toward smaller subclasses, and with less PL content within the HDL (39). Obesity was also associated with increased CETP and LCAT activities. Higher LCAT activity in obesity may form HDLs rich in cholesteryl ester, which become substrates for increased CETP activity (39). It is important to note, however, that this study assessed general obesity by BMI. Weight gain in midlife has been found to be an age-related occurrence, whereas accumulation of VAT is menopause related (40, 41); and independent of weight gain and obesity status, women transitioning through menopause accumulate more VAT in the abdomen and ectopically. This could predispose them to the alterations in HDL metabolism that were observed in this analysis. The hormonal alterations that occur around midlife may also play a role in this link. The activity of HL during the luteal phase of the menstrual cycle, or when estrogen levels are the highest, declines considerably (42), whereas increases in testosterone levels may increase HL activity (43). In SWAN HDL, we have previously shown that higher estradiol was associated with larger HDL size, large HDL-P, and HDL-CEC (44). This suggests that the decline of estrogen after menopause, and the hyperandrogenism that could accompany VAT accumulation, may enhance HL activity in women leading to smaller HDL Ps. Smaller HDL Ps, elevated Tg content, and diminished PLs in the P, in turn, could lead to detrimental effects on the CEC and function of HDL (45-47). Moreover, IR is associated with an increase in the CETP (48). This enrichment of the HDL with Tgs can also be induced by the reduction in lipoprotein lipase activity that has been observed in states of IR (49), leading to a lower cholesterol content in the HDL, as observed in our results. Further, elevated activity of hepatic triglyceride lipase and HL with IR may eventually lead to the depletion of the lipid core of the HDL conversion of HDLs into smaller Ps (34, 37, 50). Another important marker that may play a role in the association between visceral fat accumulation and HDL metrics is adiponectin. Adiponectin is an adipokine that plays an anti-inflammatory and insulin-sensitizing role. Obesity and visceral fat accumulation lead to a state of hypoadiponectinemia (51). Hypoadiponectinemia is associated with increased HL activity (52) and reduced HDL-CEC (53), indicating that the effect of visceral fat on HDL metabolism could be influenced by the role of adiponectin. Moreover, low adiponectin is associated with IR, further supporting the role of adiponectin in this relationship.

In this analysis, we show that IR mediates the detrimental effect of visceral adiposity on HDL metrics, and that controlling IR may reduce part of the effect of AT on HDL dysfunctionality. A HOMA-IR of 2.5 may clinically differentiate insulin-sensitive from IR individuals (54), which is close to the average of HOMA-IR in our sample. Thus, achieving a HOMA-IR of 2.5 in midlife women may limit the dysfunctionality in HDL that occurs with VAT accumulation. This suggests that interventions such as insulin-sensitizing agents may protect HDL against the changes in composition and function that occur with visceral fat accumulation. In vitro studies have indeed shown that metformin prevents HDL modifications and subsequent impairments in CEC (55, 56). Future clinical trials should test our hypothesis.

Despite the similarities in the links between abdominal and CV VAT depots with higher risk of cardiometabolic and CV risk factors, previous studies have suggested VAT associations with CVD risk may vary based on location, adipocyte number, size, and other factors. Human and animal studies have shown that EAT consists of smaller adipocytes and has a unique transcriptome that is enriched in genes associated with elevated inflammation (57). PAT, but not EAT, has been linked to lower estradiol concentrations (16) and to higher risk of CAC presence (17) in midlife women, suggesting that PAT is a stronger menopause-related CVD risk factor. We thus postulate that PAT may play a more substantial role in the metabolic consequences of ectopic fat accumulation compared to EAT, as evidenced by the stronger associations with HDL metrics changes and the role of IR. On the other hand, EAT may play a more localized role by factors such as inflammation on the heart compared to other CV fat depots.

The results of this study should be interpreted with caution regarding some potential limitations. We assessed the CEC only as a measure of HDL; however, visceral fat could affect other functions such as the anti-inflammatory and antioxidative functions of the HDL. Future studies should aim to assess other functions of HDL in relation to fat volumes. Even though the study was prospective, the intervals between AT and HDL metric assessment were relatively short, and thus, reverse causality cannot be ruled out. The sample size per race group is low, and we may be underpowered to detect a statistically significant difference by race. Moreover, HOMA-IR was used as a convenient and simple proxy for IR. HOMA-IR is a robust measure of IR and has good agreement, despite lower accuracy, compared to the gold-standard euglycemic-hyperinsulinemic clamp (58). However, thresholds

to determine IR have not been standardized, particularly across different sexes, races, and age groups. Compared to the excluded women, the participants included in this analysis had a higher BMI. BMI is highly and positively correlated with visceral fat, and as such, we can assume that those who were excluded had lower visceral fat accumulation. Higher BMI has been previously linked to smaller HDL size and higher concentrations of large HDL-P. In our sample, overall HDL size and large HDL-P concentrations were comparable between included and excluded women. This indicates that the exclusion of women with lower BMI may have biased the results away from the null. Moreover, we do not have data on enzymes such as CETP and LCAT activities, which could play a significant role on the associations between visceral AT and HDL metabolism. Future studies should assess the role of such markers on these associations. On the other hand, major strengths of this study include the design of the analysis by which HDL metrics were measured after the visceral fat depots, and the use of CT scans to directly quantify VAT volumes.

This is one of the first studies to investigate the associations between different VAT depots and a comprehensive HDL metric profile in midlife women. The pathways that link VAT and HDL metrics are not straightforward, especially in midlife women for whom the hormonal changes of menopause add to the complexity of these associations. In Fig. 5, we present a conceptual model that summarizes the potential pathways between AT and HDL metrics. Our results elucidate a part of the relationship, but future studies should aim to further describe the roles of other factors such as estradiol, adiponectin, and inflammation in those associations.

Our analysis shows that the abdominal and CV VAT depots predict HDL subclass distribution, size, lipid content, and potentially function 2 years later, and that IR could be of major influence on these associations. Clinically, examining the roles of modifiable risk factors that may affect VAT (such as diet and physical activity) in ameliorating the detrimental changes in HDL metrics could further elucidate the role of adiposity on HDL metabolism and future CV risk. One study has shown that a very low-calorie diet for 16 weeks reduced abdominal VAT and cardiac fat in diabetic individuals (59), whereas resistance training lowered PAT in abdominally obese participants (60). Moreover, studies on pharmaceutical interventions such as metformin, which affect IR, have shown to reduce visceral (61) and cardiac fat (62). Whether this could play a role in preventing the deleterious changes in HDL metabolism that accompany VAT accumulation should be investigated.

In summary, the present analysis shows that increased abdominal and CV AT in women during midlife may be linked to a subsequent worsening in HDL metrics, including the main antiatherogenic function of HDL in effluxing of cholesterol from macrophages in the reverse cholesterol transport process. Controlling IR during the midlife period may prevent the detrimental effect of VAT accumulation on HDL.

Acknowledgments

Clinical Centers: University of Michigan, Ann Arbor, Michigan: Carrie Karvonen-Gutierrez, principal investigator (PI) 2021 to present, Siobán Harlow, PI 2011-2021, MaryFran Sowers, PI 1994 to 2011; Massachusetts General Hospital, Boston, Massachusetts: Joel Finkelstein, PI 1999 to present; Robert Neer, PI 1994 to 1999; Rush University, Rush University Medical Center, Chicago, Illinois: Howard Kravitz, PI 2009 to present; Lynda Powell, PI 1994 to 2009; University of California, Davis, California/Kaiser: Ellen

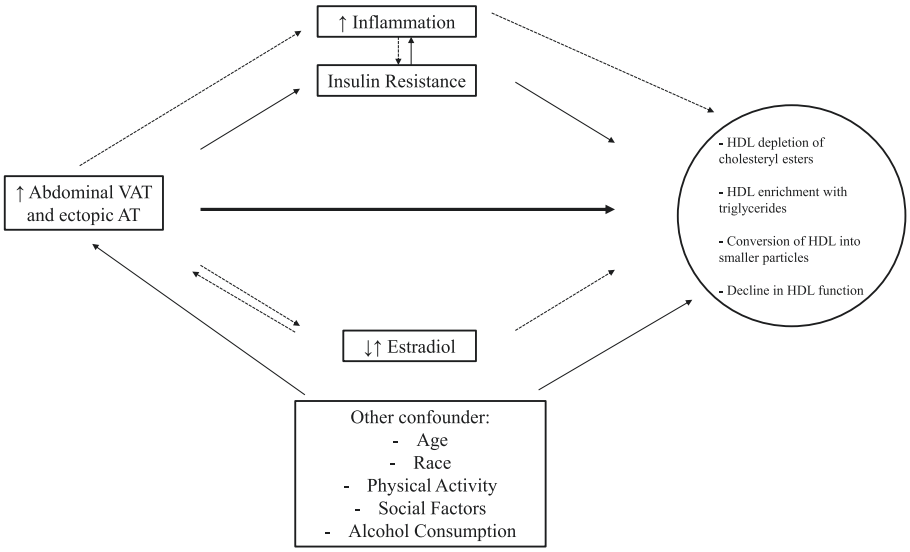

Figure 5. Conceptual model of the association between visceral adipose tissue (VAT) and high-density lipoprotein (HDL) metrics. Conceptual model for the potential pathways between VAT and HDL metabolism: Higher VAT can be linked to altered HDL metabolism through several pathways. VAT accumulation could alter HDL composition, function, and subclass distribution through its effect on enzymes involved in HDL metabolism (such as hepatic lipase [HL], cholesteryl ester transfer protein [CETP], triglyceride lipase [TGL], phospholipid-transfer protein [PLTP], and others). Other pathways could be through the induction of insulin resistance by VAT accumulation; insulin resistance could additionally alter the enzymes related to HDL metabolism. VAT accumulation is also linked to a status of chronic inflammation status, which could directly affect HDL metabolism, and that could be indirectly interrelated to the state of insulin resistance. Moreover, previous studies have shown that alterations in HDL may induce a state of chronic inflammation. In women specifically, higher VAT accumulation is linked to elevated estradiol (E2) release through conversion of androgens to estradiols. However, lower E2 during menopause could lead to higher accumulation of visceral AT. E2 is also linked independently to changes in HDL metabolism.

Gold, PI; University of California, Los Angeles, Los Angeles, California: Gail Greendale, PI; Albert Einstein College of Medicine, Bronx, New York: Carol Derby, PI 2011 to present, Rachel Wildman, PI 2010 to 2011; Nanette Santoro, PI 2004 to 2010; University of Medicine and Dentistry–New Jersey Medical School, Newark, New Jersey: Gerson Weiss, PI 1994 to 2004; and the University of Pittsburgh, Pittsburgh, Pennsylvania: Karen Matthews, PI.

National Institutes of Health (NIH) Program Office: National Institute on Aging, Bethesda, Maryland: Chhanda Dutta 2016 to present; Winifred Rossi 2012 to 2016; Sherry Sherman 1994 to 2012; Marcia Ory 1994 to 2001; National Institute of Nursing Research, Bethesda, Maryland: Program Officers.

Central Laboratory: University of Michigan, Ann Arbor, Michigan: Daniel McConnell (Central Ligand Assay Satellite Services).

SWAN Repository: University of Michigan, Ann Arbor, Michigan: Siobán Harlow 2013 to Present; Dan McConnell 2011 to 2013; MaryFran Sowers 2000 to 2011.

Coordinating Center: University of Pittsburgh, Pittsburgh, Pennsylvania: Maria Mori Brooks, PI 2012 to present; Kim Sutton-Tyrrell, PI 2001 to 2012; New England Research Institutes, Watertown, Massachusetts: Sonja McKinlay, PI 1995 to 2001.

Steering committee: Susan Johnson, current chair; Chris Gallagher, former chair.

We thank the study staff at each site and all the women who participated in SWAN.

Financial Support

This work was supported by the following: SWAN has grant support from the NIH, US Department of Health and Human Services, through the National Institute on Aging (NIA), the National Institute of Nursing Research (NINR), and the NIH Office of Research on Women's Health (ORWH) (grant Nos. U01NR004061; U01AG012505, U01AG012535, U01AG012531, U01AG012539, U01AG012546, U01AG012553, U01AG012554, and U01AG012495); the SWAN Repository (grant No. U01AG017719); the Study of Women's Health Across the Nation (SWAN) HDL ancillary study has grant support from the NIA (No. AG058690); SWAN Heart was supported by the National Heart, Lung and Blood Institute (grant Nos. HL065581 and HL065591); the SWAN Cardiovascular Fat Ancillary Study was supported by an award from the American Heart Association Great River Affiliation Clinical Research Program (No. 12CRP11900031). The content of this article is solely the responsibility of the authors and does not necessarily represent the official views of the NIA, NINR, ORWH, or the NIH.

Disclosures

A.N., K.M., I.J., E.B.M., T.J.O., J.B., N.C.W., D.M., and S.R.E. have nothing to disclose. M.M.B. serves as a Data and Safety Monitoring Board member for Cerus Corporation. D.J.R. is the founder of Vascular Strategies and serves on the Scientific Advisory Board for Alnylam, Pfizer, Novartis, and Verve.

Data Availability

Restrictions apply to the availability of some or all data generated or analyzed during this study to preserve patient confidentiality or because they were used under license. The corresponding author will on request detail the restrictions and any conditions under which access to some data may be provided. SWAN provides access to public-use data sets that include data from SWAN screening, baseline, and follow-up visits (https://agingresearchbiobank.nia.nih.gov/ and http://www.swanstudy.org/swan-research/data-access/). Investigators who require assistance accessing the public-use data set may contact the SWAN Coordinating Center (swanaccess@edc.pitt.edu). The authors declare that all supporting data are available within the article (and its data supplement).

References

1. El Khoudary SR, Aggarwal B, Beckie TM, *et al*; American Heart Association Prevention Science Committee of the Council on Epidemiology and Prevention; and Council on Cardiovascular and Stroke Nursing. Menopause transition and cardiovascular disease risk: implications for timing of early prevention: a scientific statement from the American Heart Association. *Circulation*. 2020;142(25):e506-e532.
2. Matthews KA, Crawford SL, Chae CU, *et al*. Are changes in cardiovascular disease risk factors in midlife women due to chronological aging or to the menopausal transition? *J Am Coll Cardiol*. 2009;54(25):2366-2373.
3. El Khoudary SR. HDL and the menopause. *Curr Opin Lipidol*. 2017;28(4):328-336.
4. von Eckardstein A, Nofer JR, Assmann G. High density lipoproteins and arteriosclerosis. Role of cholesterol efflux and reverse cholesterol transport. *Arterioscler Thromb Vasc Biol*. 2001;21(1):13-27.
5. Eapen DJ, Kalra GL, Rifai L, Eapen CA, Merchant N, Khan BV. Raising HDL cholesterol in women. *Int J Womens Health*. 2010;1:181-191.
6. El Khoudary SR, Chen X, Nasr A, *et al*. HDL (high-density lipoprotein) subclasses, lipid content, and function trajectories across the menopause transition: SWAN-HDL Study. *Arterioscler Thromb Vasc Biol*. 2021;41(2):951-961.
7. El Khoudary SR, Ceponiene I, Samargandy S, *et al*. HDL (high-density lipoprotein) metrics and atherosclerotic risk in women. *Arterioscler Thromb Vasc Biol*. 2018;38(9):2236-2244.
8. Holmes MV, Millwood IY, Kartsonaki C, *et al*; China Kadoorie Biobank Collaborative Group. Lipids, lipoproteins, and metabolites and risk of myocardial infarction and stroke. *J Am Coll Cardiol*. 2018;71(6):620-632.
9. Agarwala AP, Rodrigues A, Risman M, *et al*. High-density lipoprotein (HDL) phospholipid content and cholesterol efflux capacity are reduced in patients with very high HDL cholesterol and coronary disease. *Arterioscler Thromb Vasc Biol*. 2015;35(6):1515-1519.
10. Khera AV, Cuchel M, de la Llera-Moya M, *et al*. Cholesterol efflux capacity, high-density lipoprotein function, and atherosclerosis. *N Engl J Med*. 2011;364(2):127-135.
11. Mora S, Otvos JD, Rifai N, Rosenson RS, Buring JE, Ridker PM. Lipoprotein particle profiles by nuclear magnetic resonance compared with standard lipids and apolipoproteins in predicting incident cardiovascular disease in women. *Circulation*. 2009;119(7):931-939.
12. van der Steeg WA, Holme I, Boekholdt SM, *et al*. High-density lipoprotein cholesterol, high-density lipoprotein particle size, and apolipoprotein A-I: significance for cardiovascular risk: the IDEAL and EPIC-Norfolk studies. *J Am Coll Cardiol*. 2008;51(6):634-642.
13. Mora S, Glynn RJ, Ridker PM. High-density lipoprotein cholesterol, size, particle number, and residual vascular risk after potent statin therapy. *Circulation*. 2013;128(11):1189-1197.
14. Lovejoy JC, Champagne CM, de Jonge L, Xie H, Smith SR. Increased visceral fat and decreased energy expenditure during the menopausal transition. *Int J Obes (Lond)*. 2008;32(6):949-958.
15. Samargandy S, Matthews KA, Brooks MM, *et al*. Abdominal visceral adipose tissue over the menopause transition and

carotid atherosclerosis: the SWAN Heart study. *Menopause*. 2021;28(6):626-633.
16. El Khoudary SR, Shields KJ, Janssen I, *et al*. Cardiovascular fat, menopause, and sex hormones in women: the SWAN Cardiovascular Fat ancillary study. *J Clin Endocrinol Metab*. 2015;100(9):3304-3312.
17. El Khoudary SR, Shields KJ, Janssen I, *et al*. Postmenopausal women with greater paracardial fat have more coronary artery calcification than premenopausal women: the study of Women's Health Across the Nation (SWAN) Cardiovascular Fat ancillary study. *J Am Heart Assoc*. 2017;6(2):e004545.
18. Nicklas BJ, Penninx BW, Ryan AS, Berman DM, Lynch NA, Dennis KE. Visceral adipose tissue cutoffs associated with metabolic risk factors for coronary heart disease in women. *Diabetes Care*. 2003;26(5):1413-1420.
19. Rashid S, Watanabe T, Sakaue T, Lewis GF. Mechanisms of HDL lowering in insulin resistant, hypertriglyceridemic states: the combined effect of HDL triglyceride enrichment and elevated hepatic lipase activity. *Clin Biochem*. 2003;36(6):421-429.
20. Serra MC, Ryan AS, Sorkin JD, Favor KH, Goldberg AP. High adipose LPL activity and adipocyte hypertrophy reduce visceral fat and metabolic risk in obese, older women. *Obesity (Silver Spring)*. 2015;23(3):602-607.
21. Sowers MFR, Crawford S, Sternfeld B, *et al*. SWAN: a multicenter, multiethnic, community-based cohort study of women and the menopausal transition. In: Lobo RA, Kelsey J, Marcus R, eds. *Menopause: Biology and Pathology*. Academic Press; 2000:175-180.
22. Thurston RC, Sowers MR, Sutton-Tyrrell K, *et al*. Abdominal adiposity and hot flashes among midlife women. *Menopause*. 2008;15(3):429-434.
23. Shields KJ, Barinas-Mitchell E, Gingo MR, *et al*. Perivascular adipose tissue of the descending thoracic aorta is associated with systemic lupus erythematosus and vascular calcification in women. *Atherosclerosis*. 2013;231(1):129-135.
24. Jeyarajah EJ, Cromwell WC, Otvos JD. Lipoprotein particle analysis by nuclear magnetic resonance spectroscopy. *Clin Lab Med*. 2006;26(4):847-870.
25. Warnick GR, Albers JJ. A comprehensive evaluation of the heparin-manganese precipitation procedure for estimating high density lipoprotein cholesterol. *J Lipid Res*. 1978;19(1):65-76.
26. Steiner P, Freidel J, Bremner W, Stein E. Standardization of micromethods for plasma cholesterol, triglyceride and HDL-cholesterol with the Lipid Clinics' methodology. *J Clin Chem Clin Biochem*. 1981;19(8):850.
27. Ainsworth BE, Sternfeld B, Richardson MT, Jackson K. Evaluation of the Kaiser Physical Activity Survey in women. *Med Sci Sports Exerc*. 2000;32(7):1327-1338.
28. Nasr A, Matthews K, Janssen I, *et al*. *Supplementary data for "Associations of abdominal and cardiovascular adipose tissue depots with HDL metrics in midlife women: The SWAN Study." Inter-university Consortium for Political and Social Research*. 2022. Accessed February 04, 2022. https://www.openicpsr.org/openicpsr/project/161441/version/V1/view
29. Neeland IJ, Ayers CR, Rohatgi AK, *et al*. Associations of visceral and abdominal subcutaneous adipose tissue with markers of cardiac and metabolic risk in obese adults. *Obesity (Silver Spring)*. 2013;21(9):E439-E447.
30. Sam S, Haffner S, Davidson MH, *et al*. Relationship of abdominal visceral and subcutaneous adipose tissue with lipoprotein particle number and size in type 2 diabetes. *Diabetes*. 2008;57(8):2022-2027.
31. Woudberg NJ, Lecour S, Goedecke JH. HDL subclass distribution shifts with increasing central adiposity. *J Obes*. 2019;2019:2107178.
32. Ong KL, Ding J, McClelland RL, *et al*. Relationship of pericardial fat with lipoprotein distribution: the Multi-Ethnic Study of Atherosclerosis. *Atherosclerosis*. 2015;241(2):664-670.
33. Huang G, Wang D, Zeb I, *et al*. Intra-thoracic fat, cardiometabolic risk factors, and subclinical cardiovascular disease in healthy, recently menopausal women screened for the Kronos Early Estrogen Prevention Study (KEEPS). *Atherosclerosis*. 2012;221(1):198-205.
34. Rashid S, Genest J. Effect of obesity on high-density lipoprotein metabolism. *Obesity (Silver Spring)*. 2007;15(12):2875-2888.
35. Shen GX, Zhang JY, Blanchard R, *et al*. Analysis of cholesteryl ester transfer activity in adipose tissue. *Int J Obes Relat Metab Disord*. 1996;20(Suppl 3):S114-S120.
36. Patsch JR, Karlin JB, Scott LW, Smith LC, Gotto AM Jr. Inverse relationship between blood levels of high density lipoprotein subfraction 2 and magnitude of postprandial lipemia. *Proc Natl Acad Sci U S A*. 1983;80(5):1449-1453.
37. Tchernof A, Després JP. Pathophysiology of human visceral obesity: an update. *Physiol Rev*. 2013;93(1):359-404.
38. Dobiásová M, Frohlich J. Understanding the mechanism of LCAT reaction may help to explain the high predictive value of LDL/HDL cholesterol ratio. *Physiol Res*. 1998;47(6):387-397.
39. Stadler JT, Lackner S, Mörkl S, *et al*. Obesity affects HDL metabolism, composition and subclass distribution. *Biomedicines*. 2021;9(3):242.
40. Matthews KA, Abrams B, Crawford S, *et al*. Body mass index in mid-life women: relative influence of menopause, hormone use, and ethnicity. *Int J Obes Relat Metab Disord*. 2001;25(6):863-873.
41. Thurston RC, Karvonen-Gutierrez CA, Derby CA, El Khoudary SR, Kravitz HM, Manson JE. Menopause versus chronologic aging: their roles in women's health. *Menopause*. 2018;25(8):849-854.
42. Tikkanen MJ, Kuusi T, Nikkilä EA, Stenman UH. Variation of postheparin plasma hepatic lipase by menstrual cycle. *Metabolism*. 1986;35(2):99-104.
43. Sorva R, Kuusi T, Dunkel L, Taskinen MR. Effects of endogenous sex steroids on serum lipoproteins and postheparin plasma lipolytic enzymes. *J Clin Endocrinol Metab*. 1988;66(2):408-413.
44. El Khoudary SR, Nasr A, Billheimer J, *et al*. Associations of endogenous hormones with HDL novel metrics across the menopause transition: the SWAN HDL study. *J Clin Endocrinol Metab*. 2022;107(1):e303-e314.
45. de la Llera-Moya M, Drazul-Schrader D, Asztalos BF, Cuchel M, Rader DJ, Rothblat GH. The ability to promote efflux via ABCA1 determines the capacity of serum specimens with similar high-density lipoprotein cholesterol to remove cholesterol from macrophages. *Arterioscler Thromb Vasc Biol*. 2010;30(4):796-801.
46. Nakanishi S, Vikstedt R, Söderlund S, *et al*. Serum, but not monocyte macrophage foam cells derived from low HDL-C subjects, displays reduced cholesterol efflux capacity. *J Lipid Res*. 2009;50(2):183-192.
47. Greene DJ, Skeggs JW, Morton RE. Elevated triglyceride content diminishes the capacity of high density lipoprotein to deliver cholesteryl esters via the scavenger receptor class B type I (SR-BI). *J Biol Chem*. 2001;276(7):4804-4811.
48. de Vries R, Borggreve SE, Dullaart RPF. Role of lipases, lecithin:cholesterol acyltransferase and cholesteryl ester transfer protein in abnormal high density lipoprotein metabolism in insulin resistance and type 2 diabetes mellitus. *Clin Lab*. 2003;49(11-12):601-613.
49. Garg A. Insulin resistance in the pathogenesis of dyslipidemia. *Diabetes Care*. 1996;19(4):387-389.
50. Syvänne M, Ahola M, Lahdenperä S, *et al*. High density lipoprotein subfractions in non-insulin-dependent diabetes mellitus and coronary artery disease. *J Lipid Res*. 1995;36(3):573-582.
51. Drolet R, Bélanger C, Fortier M, *et al*. Fat depot-specific impact of visceral obesity on adipocyte adiponectin release in women. *Obesity (Silver Spring)*. 2009;17(3):424-430.
52. Schneider JG, von Eynatten M, Schiekofer S, Nawroth PP, Dugi KA. Low plasma adiponectin levels are associated with increased hepatic lipase activity in vivo. *Diabetes Care*. 2005;28(9):2181-2186.
53. Marsche G, Zelzer S, Meinitzer A, *et al*. Adiponectin predicts high-density lipoprotein cholesterol efflux capacity in adults irrespective of body mass index and fat distribution. *J Clin Endocrinol Metab*. 2017;102(11):4117-4123.
54. Tang Q, Li X, Song P, Xu L. Optimal cut-off values for the Homeostasis Model Assessment of Insulin Resistance (HOMA-IR) and pre-diabetes screening: developments in research and prospects for the future. *Drug Discov Ther*. 2015;9(6):380-385.

55. Matsuki K, Tamasawa N, Yamashita M, *et al*. Metformin restores impaired HDL-mediated cholesterol efflux due to glycation. *Atherosclerosis*. 2009;206(2):434-438.
56. Machado AP, Pinto RS, Moysés ZP, Nakandakare ER, Quintão EC, Passarelli M. Aminoguanidine and metformin prevent the reduced rate of HDL-mediated cell cholesterol efflux induced by formation of advanced glycation end products. *Int J Biochem Cell Biol*. 2006;38(3):392-403.
57. Marchington JM, Pond CM. Site-specific properties of pericardial and epicardial adipose tissue: the effects of insulin and high-fat feeding on lipogenesis and the incorporation of fatty acids in vitro. *Int J Obes*. 1990;14(12):1013-1022.
58. Bonora E, Targher G, Alberiche M, *et al*. Homeostasis model assessment closely mirrors the glucose clamp technique in the assessment of insulin sensitivity: studies in subjects with various degrees of glucose tolerance and insulin sensitivity. *Diabetes Care*. 2000;23(1):57-63.
59. Snel M, Jonker JT, Hammer S, *et al*. Long-term beneficial effect of a 16-week very low calorie diet on pericardial fat in obese type 2 diabetes mellitus patients. *Obesity (Silver Spring)*. 2012;20(8):1572-1576.
60. Christensen RH, Wedell-Neergaard AS, Lehrskov LL, *et al*. Effect of aerobic and resistance exercise on cardiac adipose tissues: secondary analyses from a randomized clinical trial. *JAMA Cardiol*. 2019;4(8):778-787.
61. Tokubuchi I, Tajiri Y, Iwata S, *et al*. Beneficial effects of metformin on energy metabolism and visceral fat volume through a possible mechanism of fatty acid oxidation in human subjects and rats. *PLoS One*. 2017;12(2):e0171293.
62. Ziyrek M, Kahraman S, Ozdemir E, Dogan A. Metformin monotherapy significantly decreases epicardial adipose tissue thickness in newly diagnosed type 2 diabetes patients. *Rev Port Cardiol (Engl Ed)*. 2019;38(6):419-423.